Title page

Analysis of modular gene co-expression networks reveals molecular pathways underlying Alzheimer's disease and progressive supranuclear palsy

Lukas Iohan Carvalho[1,2], Jean-Charles Lambert[3], Marcos R. Costa[1,3,*]

1. Brain Institute, Federal University of Rio Grande do Norte, Natal, Brazil
2. Bioinformatics Multidisciplinary Environment, Federal University of Rio Grande do Norte, Natal, Brazil
3. Univ. Lille, Inserm, CHU Lille, Institut Pasteur de Lille, U1167-RID-AGE facteurs de risque et déterminants moléculaires des maladies liées au vieillissement, DISTALZ, Lille, France

*Corresponding author

Correspondence should be addressed to:

Marcos Costa, MD, PhD

INSERM UMR1167

Institut Pasteur de Lille

1 rue du Pr. Calmette

59019 Lille cedex, France

Tel: 00 33 (0)3 20 87 77 10

marcos.costa@pasteur-lille.fr

Abstract

A comprehensive understanding of the pathological mechanisms involved at different stages of neurodegenerative diseases is key for the advance of preventive and disease-modifying treatments. Gene expression alterations in the diseased brain is a potential source of information about biological processes affected by pathology. In this work, we performed a systematic comparison of gene expression alterations in the brains of human patients diagnosed with Alzheimer's disease (AD) or Progressive Supranuclear Palsy (PSP) and animal models of amyloidopathy and tauopathy. Using system biology approaches to uncover biological processes associated with gene expression alterations, we could pinpoint processes more strongly associated with tauopathy/PSP and amyloidopathy/AD. Notably, our data reveal that gene expression alterations related to immune-inflammatory responses preponderate in younger, whereas those associated to synaptic transmission are mainly observed in older AD patients. In PSP, however, changes associated with immune-inflammatory responses and synaptic transmission overlap. These two different patterns observed in AD and PSP brains are fairly recapitulated in animal models of amyloidopathy and tauopathy, respectively. Moreover, in AD, but not PSP or animal models, gene expression alterations related to RNA splicing are highly prevalent, whereas those associated with myelination are enriched both in AD and PSP, but not in animal models. Finally, we identify 12 AD and 4 PSP genetic risk factors in cell-type specific co-expression modules, thus contributing to unveil the possible role of these genes to pathogenesis.

Introduction

Alzheimer's disease (AD) and progressive supranuclear palsy (PSP) are incurable neurodegenerative disorders that share some common pathological hallmarks, such as synapse loss and the presence of intraneuronal neurofibrillary tangles (NFTs) composed of hyperphosphorylated microtubule-associated protein tau (MAPT or TAU) [1, 2]. AD is also characterized by extracellular amyloid plaques composed of aggregated amyloid-beta peptides and a sustained immune inflammatory response leading to the activation of the brain's resident macrophages (microglia) and other immune cells [3, 4]. Although these neuropathological features of AD and PSP have been extensively described in post-mortem brain samples, their precise contribution to pathogenesis remains poorly understood. Recently, RNA-sequencing in large sample cohorts have been used to identify alterations in gene expression associated with onset and progression of AD and PSP [5]. However, no direct comparison of the transcriptional signatures in the brains affected by these two neuropathologies has been performed.

Animal models of tau and amyloid pathology have been largely used to probe AD-related processes [6] and identify gene expression alterations associated with those two different pathological hallmarks [7, 8, 9, 10, 11, 12]. Interestingly, it has been reported that transcriptional perturbations observed in the AD human brain overlap with gene expression alterations observed in the brain of mouse models of AD, frontotemporal dementia, Huntington's disease, amyotrophic lateral sclerosis and aging [7, 8, 12, 13]. These observations suggest that transcriptional changes in the diseased brain could outline pathophysiological processes and therefore contribute to the understanding of disease mechanisms. However, it remains unclear whether amyloid and tau pathology could lead to similar or distinct transcriptional alterations in the human brain.

In this study, we hypothesized that studying the transcriptome of brain samples obtained from *postmortem* AD and PSP patients, as well as in animal models, could help to disentangle gene expression alterations associated with amyloid versus tau pathology. To that, we systematically probed gene expression alterations in the temporal cortex and cerebellum of AD and PSP patients [5], as well as in two different transgenic mouse models used to study amyloid or tau pathology, using different bioinformatics approaches. We also evaluated gene expression at the transcript level, allowing the identification of both differentially expressed genes (DEGs) and genes with different transcript usage (gDTUs) or isoform switches [14].

Our results suggest that inflammatory response is more strongly associated with amyloid pathology and predominates in the brain of AD patients younger than 80 years. Conversely, synaptic alterations are observed both in young PSP and old AD patients and correlates with tau pathology. Interestingly, we show that isoform switches are abundant in the AD and PSP human brain, but rare in animal models of both amyloid and tau pathology, suggesting that alterations in alternative splicing can be a specific feature of the diseased human brain. Altogether, our work improves our understanding

about the biological processes affected by amyloid versus tau pathology and contributes for the development of precise disease-modifying strategies.

Results

Gene expression alterations in the neocortex of AD and PSP patients

To investigate the similarities and differences in gene expression alterations in the brain of patients with AD or PSP, we analyzed transcriptome data for Cerebellum (CBE) and Temporal cortex (TCX) samples from North American Caucasian subjects with neuropathological diagnosis of AD, PSP or elderly controls without clinic-pathological signs of neurodegenerative diseases [5]. We subdivided samples per age (Table 1), which is the only metadata common to the different groups of patients and strongly correlates with pathological progression both in AD and PSP [15, 16]. We observed that both the number of differentially expressed genes (DEGs) and genes with differential transcript usage (gDTUs) detected in the TCX of AD patients compared to controls increased with age (Figure 2). Notably, there was very little overlap in the DEGs and gDTUs observed at different ages, suggesting that singular gene expression alterations prevail in the AD brain at distinct pathological stages (Figure S1, Table S1). Accordingly, gene set enrichment analysis (GSEA) revealed that DEGs and gDTUs identified in the AD TCX were significantly enriched for distinct gene ontologies (GOs) according to age (Figure 2A, Table S2). While significant enrichment for GOs associated with immune-inflammatory response, RNA splicing, BMP signaling pathway, gliogenesis and regulation of neuron projection development were already observed in group A and remained in groups B and C, terms associated with ion homeostasis, Wnt signaling pathway, cellular response to lipid were exclusively detected in group B. The terms cellular respiration, protein targeting to ER and regulation of protein catabolic processes were solely observed in group C, whereas terms related to synapse signaling were mainly observed in groups B and C. As previously reported, enrichment for the latter terms was only observed when inputting gDTUs alone or in combination with DEGs (Figure 2A), supporting the view that isoform-switches are an important source of gene expression alterations affecting synapses [14]. Analyses of gene expression alterations in the cerebellum of the same patients also revealed a weak overlap among DEGs and gDTUs observed at different ages (Figure S1). Yet, DEGs and gDTUs in all groups were enriched for GOs associated with regulation of neuron projection development, synapse signaling, mRNA metabolic processes and RNA splicing (Figure S2), as observed in the TCX (Figure 2A). These observations suggest that some biological processes are commonly altered in the TCX and cerebellum of AD patients, whereas others, such as immune-inflammatory response, ion homeostasis, BMP and Wnt signaling pathways are mainly affected in the TCX.

In contrast with AD brains, where few DEGs could be detected at early ages, we found a high number of DEGs and gDTUs in the TCX of PSP patients in group A, consistent with the fast progression of this disease [17]. In this group, DEGs and gDTUs were significantly enriched for several GOs observed in AD patients including those associated with synapse signaling, immune system process, ion homeostasis and regulation of neuron projection development (Figure 2B, Table S2). The number of

DEGs and gDTUs identified in elderly PSP patients (group B) was significantly lower than in group A and did not show any enrichment for GOs (Figure 2B). This could be due to the reduced number of samples in group B or to a lower pathological burden in the neocortex of these PSP patients, reflecting the clinical heterogeneity of PSP [18]. According to this second possibility, we observed an inverted pattern in the distribution of DEGs and gDTUs in the cerebellum of PSP patients, namely a higher number of altered genes in group B (Figure S1). However, only DEGs/gDTUs from group A showed significant enrichment in GSEA (Figure S2B). Some enriched GOs observed in the cerebellum were also detected in the TCX, such as ion homeostasis and regulation of neuron projection development but did not show any enrichment for terms related to immune system processes (Figure S2A). Together with our observations in AD patients, these observations suggest that gene expression alterations associated with immune-inflammatory response are mainly restricted to the neocortex of both AD and PSP patients.

Gene network analyses reveal cell-type specific molecular pathways in AD and PSP

To further exploit transcriptomic data obtained from in AD and PSP patients and uncover the latent systems-level functionality of genes, we analyzed modular gene co-expression networks using CEMiTool [19]. We detected eight different modules in the TCX of AD and PSP individuals (Figure 3A). Modules 1 and 2 in AD (M1_AD and M2_AD) and modules 1 and 3 in PSP (M1_PSP and M3_PSP) were significantly enriched for genes associated with synaptic signaling. M3_AD and M2_PSP were significantly enriched for myelination, whereas M5_AD, M8_AD, M4_PSP and M8_PSP were significantly enriched for several terms associated with immune-inflammatory processes. The modules M6_AD, M7_AD and M6_PSP were associated with extracellular matrix and cell differentiation/angiogenesis, whereas M4_AD and M5_PSP were associated with cellular response to growth factors. In PSP, we also detected a module associated with apoptosis (M7).

Next, we used Cell-ID [20] to identify cell-types of the adult human brain enriched for the gene signatures identified in the different modules. We first performed multiple correspondence analysis (MCA) in single-cell RNA-seq (scRNA-seq) data obtained from the entorhinal cortex of 3 healthy (Braak 0) individuals [21] (Figure 3B). Next, we used Cell-ID to extract and calculate the enrichment of per-cell gene signatures using as reference (i) list of genes in each module and (ii) per-cell gene signatures extracted through Cell-ID from scRNA-seq data. We observed that modules associated with synapses were mainly enriched in glutamatergic neurons, whereas those associated with myelination were consistently enriched in oligodendrocytes (Figure 3A, Figure3C). M5_AD and M4_PSP were exclusively enriched in microglial cells, consistent with their enrichment for immune-inflammatory processes. However, M8 in both AD and PSP, which was also associated with inflammation, showed a significant enrichment in astrocytes. These cells were also significantly enriched for M4_AD and M5_PSP (cellular response to growth factors) and M7_PSP (apoptosis). Finally, we found a

significant enrichment of M6_AD, M7_AD and M6_PSP gene signatures in endothelial cells.

Activity of modules is differently altered in AD and PSP brains

Next, using the fgsea (Fast Gene Set Enrichment Analysis) package [22] built-in CEMitool, we analyzed the association of module activity to sample phenotypes. In this analysis, genes from co-expression modules are treated as gene sets and the z-score normalized expression of the samples within each phenotype is ranked, providing an assessment of modules across different phenotypes [19]. We observed that the normalized enrichment score (NES) of M4, M6, M7 and M8 was greatly higher in AD patients, whereas activity of M1 and M3 was higher in PSP patients compared to control subjects (Figure 4A). Conversely, NES of M2, M4, M6, M7 and M8 in PSP and M1, M2 and M3 in AD brains was marginally lower than in controls (Figure 4B). These findings suggest that gene expression alterations associated with the immune-inflammatory system, cellular response to growth factors, extracellular matrix and cell differentiation/angiogenesis predominate in AD, whereas those associated with synapses and myelination prevail in PSP. According to this interpretation, quantification of the proportion of genes with altered expression within modules revealed that DEGs/gDTUs were more numerous in synaptic modules of PSP than in AD (Figure 4C). Interestingly, genes with altered expression in these synaptic modules were mainly detected at older ages (groups B and C) in AD brains (Figure 4). Conversely, the frequency of DEGs/gDTUs in modules associated with extracellular matrix, cell differentiation/angiogenesis and response to growth factors was much higher in AD than in PSP brains. The modules associated with myelination and immune-inflammatory responses showed a high proportion of DEGs/gDTUs in both diseases and they were highly frequent at early ages (Figure 4C).

Next, we analyzed RNAseq data from the Mount Sinai/JJ Peters VA Medical Center Brain Bank (MSBB–Mount Sinai NIH Neurobiobank) cohort [23]. Using this dataset to compare transcriptional signatures of different brain regions, we have previously shown that gene expression alterations are more prominent in the Broadmann area (BA) 36 of the temporal lobe than in the BA10 of the frontal lobe of AD patients (Marques-Coelho et al., 2021). This pattern tightly correlates with pathological progression indicated by Braak stages [24]. Using CEMItool, we identified 4 gene co-expression modules both in BA10 and BA36 (Figure S3A, Table S3). Interestingly, activity of M2 in BA10 was higher in AD patients and genes in this module significantly enriched for GOs associated with immune-inflammatory responses (Figure S3B). In this same brain region, no modules associated with synapses could be identified (Table S3). Conversely, M1 and M2 in BA36 enriched for several synapse related GOs and showed a weaker activity in AD patients compared to controls (Figure S3C, Table S3). Collectively, our observations in two different datasets using CEMitool suggest that transcriptional alterations related to immune-inflammatory processes are an early event in the pathogenesis of AD, whereas gene expression changes related to synapses are a late outcome.

Temporal gene expression alterations in 5XFAD and TauD35 mice

To further investigate the correlation between pathological progress and gene expression alterations, we took advantage of RNA-seq data generated from the brain of animal models of β-amyloidopathy (5XFAD) and tauopathy (TauD35) at different ages (Table 3). Considering that PSP is primarily a tauopathy, whereas AD combines features of β-amyloidopathy and tauopathy, we hypothesized that study of these two different animal models could help to uncover pathological processes associated with those hallmarks. Similar to what we observed in the brains of AD patients, the number of DEGs drastically increased with age/pathology progression in both 5XFAD and TauD35 mouse models (Figure 5). Interestingly, however, the number of gDTUs remained low in both models, suggesting that alterations in alternative splicing mechanisms are uncommon in animal models of both β-amyloidopathy and tauopathy. GO analyses revealed that DEGs in 5XFAD mice were enriched for many terms previously observed in the brain of AD patients, such as immune system response, ion homeostasis, response to hormone stimulus, MAPK cascade and synapse signaling (Figure 5A). Also, like AD brains, DEGs were enriched for terms associated with immune-inflammatory response at early pathological stages (4 and 12 months), whereas only at 18 months DEGs were enriched for synapse signaling ontologies. Strikingly, this pattern was upturned in the brains of Taud35 mice (Figure 5B). While at 4 months DEGs/gDTUs were significantly enriched for synapse signaling, only at 17 months they were so for immune system processes.

Next, using gene co-expression networks, we identified a module (M1) associated with immune system response in both animal models (Figure 6C) and this module showed higher activity in mutants compared to controls (Figure 6A). Notably, while several DEGs/gDTUs could be detected in the M1 of 5XFAD mice at early stages of pathology (4 months), the vast majority of DEGs in the M1 of Taud35 mice were detected only at late stages (Figure 6B). Conversely, the activity of the modules associated with synapse signaling in 5XFAD mice (M7 and M8) did not show any difference between mutants and controls (Figure 6A). Yet, like human AD brains, DEGs identified in these modules were mainly observed in old animals – 18 months (Figure 6B). Also analogous to human AD and PSP patients, modules associated with extracellular matrix in both animal models (M1_TauD35 and M5_5XFAD) showed higher activity in mutants. On the other hand, we could not detect modules associated with myelination or RNA-splicing in both animal models. Altogether, these findings suggest that β-amyloidopathy primarily leads to an immune-inflammatory response with secondary effects on synapse signaling, whereas tauopathy chiefly affect synapses with subsequent effects in immune-inflammatory activation.

AD and PSP susceptibility genes are linked to specific gene co-expression networks

Genome-wide association studies (GWAS) have identified polymorphisms in or near several genes that are associated with AD or PSP risk [25, 26, 27]. We used CEMitool to visualize the interactions between these risk genes and the co-expression modules

identified in each pathology (Figure 7). In AD modules, we found WNT3 and PLCG2 in M1, ABCA1, CR1 and PTK2B in M2, CSTH and EGFR in M4, and HLA-DRA, INPP5D, TREM1 and TREM2 in M5 (Figure 7A). In PSP modules (Figure 7B), we could observe PTPRT in M1 and MOBP, SEMA4D and SLCO1A2 in M2. Together with our previous findings, these results suggest that those AD risk factors may contribute to pathogenesis through regulation of synaptic transmission in glutamatergic neurons, immune-inflammatory response in microglia and response to growth factors in astrocytes, whereas PSP risk factors chiefly modulate synaptic transmission and myelination.

Discussion

Understanding the progression of pathological events in the brain of patients affected by neurodegenerative diseases may help to identify preventive and prognostic-changing treatments for these conditions. In this work, we combined the analysis of transcriptomic data generated from the human brain and a system biology approach to identify similarities and discrepancies in the biological processes affected in patients diagnosed with two different neurodegenerative diseases. PSP is a primary tauopathy with abnormal accumulation of tau protein within neurons as neurofibrillary tangles (NFTs), primarily in the basal ganglia, diencephalon, brainstem, and cerebellum, with restricted involvement of the neocortex [28]. On the other hand, AD can be considered as a secondary tauopathy, since Aβ plaques are closely tied to the primary neuropathological process. Our findings suggest that, at early ages/stages of disease, tauopathy would be primarily associated with alterations in synaptic signaling processes, whereas amyloidopathy would be mainly associated with immune-inflammatory responses in the brain of PSP and AD patients, respectively. Accordingly, in mouse models of tauopathy and amyloidopathy, gene expression alterations associated with synaptic or immune-inflammatory processes, respectively, predominate at early stages of pathology progression. Last, but not least, we also identify AD risk genes in co-expression modules associated with those biological processes, thus shedding light on their possible contribution to disease onset/progression.

In this study, we analyzed RNAseq data generated from PSP patients showing neuropathological signs of tauopathy in the temporal lobe (Braak stages 1-3, when NFTs are already distinguished the trans-entorhinal and entorhinal cortices - ref) and AD patients with widespread NFTs in the mesocortex, allocortex and neocortex (Braak stages 5-6). Therefore, we believe that the gene expression profile of these samples represents a reasonable proxy of tauopathy- and mixed tauopathy/amyloidopathy-related biological processes altered in the brains of PSP and AD patients, respectively. Additionally, the analysis of RNAseq data obtained from the brains of animal models of tauopathy and amyloidopathy with a well-characterized time progression of pathological processes, allows a more suitable identification of gene expression alterations primarily associated with those processes.

Our observations both in the brain of human patients with PSP and mouse model of tauopathy suggest that biological processes associated with tau accumulation mainly involve neuronal synaptic transmission and that activation of immune-inflammatory processes could be a secondary response. Conversely, in the brain of AD patients and mouse model of amyloidopathy, alterations in gene expression associated with immune-inflammatory response seem to precede those related with synapse signaling. These findings are in agreement with previous work using co-expression modules to identify possible overlaps between transcriptional alteration in the AD brain and in mouse models of tauopathy or amyloidopathy [13, 10, 7, 8, 9] and may suggest that alterations in synaptic transmission and immune-inflammatory responses are interconnected in a

positive feedback loop with different entry points depending on the predominance of tauopathy and amyloidopathy in the brain.

We also show that some biological processes are particularly affected in the brain of AD patients and cannot be fully recapitulated in animal models. This is particularly evident for gene expression alterations associated with RNA splicing processes, which could explain the high number of genes with isoform switches observed in the brains of AD patients [29, 14]. Conversely, gene expression alterations associated with ion homeostasis, response to hormone stimuli, angiogenesis, regulation of protein catabolism, bioenergetics and MAPK cascade were observed both in AD human brains and in 5XFAD mice, but not TauD35 mice, suggesting a link between amyloidopathy and those biological processes. These observations are in accordance with previous work in mice and humans [8, 9, 14] and further support the notion that analysis of gene expression profiles in neurodegenerative diseases is a powerful tool to identify pathology-related alterations.

Our results also show that gene expression alterations associated with myelination, response to growth hormones and angiogenesis could be identified, respectively, in oligodendrocytes, astrocytes and endothelial cells both in AD and PSP brains, suggesting that these biological processes could be common to both pathologies. However, our data indicate that changes in myelination are more prominent in PSP, as it has been previously shown using Weighted Gene Co-Expression Network Analysis [30]. On the other hand, the astrocyte module associated with response to growth factors was significantly affected in AD, but not in PSP brains where we could identify an enrichment for the astrocyte module associated with apoptosis. These alterations could suggest that reactive astrogliosis in AD and PSP are distinct, likely due to the early Tau accumulation in astrocytes in the latter [31].

The co-expression of susceptibility genes in cell-type specific modules of AD and PSP revealed in this work is also an interesting hint about the biological processes regulated by those genes. Indeed, we confirm the known roles of INPP5D and TREM2 in the regulation of microglial activation in AD [32, 33] and the involvement of MOBP and SEMA4D in myelinating oligodendrocytes in PSP [30, 34, 35]. Additionally, we provide some interesting hits on the possible contribution of PLCG2, WNT3, ABCA1, CR1 and PTK2B for the regulation of synapse-related processed in glutamatergic neurons, as well as CSTH and EGFR for the regulation of reactive astrogliogenesis in AD. Moreover, we show evidence suggesting that SLCO1A2 and PTRPT contribute to PSP pathogenesis by regulating myelination and synaptic transmission, respectively.

Altogether, our work contributes to identify pathological processes primarily associated with amyloidopathy and tauopathy in neurodegenerative diseases, as well as reveal common pathological processes likely resulting from glial and vascular responses.

Methods

Bulk RNAseq data from human and animal models

All RNAseq datasets used in this work were from AMP-AD Knowledge Portal (https://www.synapse.org) following all terms and conditions to the use of the data. From Mayo Clinic Alzheimer's Disease Genetics Studies (Mayo), we analyzed RNAseq data generated from two areas (Temporal Cortex and Cerebellum) and 3 types of subjects: individuals with Alzheimer's Disease; Progressive Supranuclear Palsy: and elderly individuals with no neurodegenerative disease. To classify the subjects in control (elderly individuals with no neurodegenerative disease) or with one of the two conditions mentioned above we used column 'Group' column from metadata obtained from the AMP-AD Knowledge portal (table 1). The "Age_Group" column was used to divide individuals into three groups: A, age of death between 70 and 80 years old, including these two ages; B, age of death between 81 and 89, including these two ages; and C, age of death equal or superior to 90 years old. In RNAseq data from Temporal Cortex, individuals with Alzheimer's Disease have *N = 75* subjects (A = 18, B = 37 and C = 20); individuals with Progressive Supranuclear Palsy have *N = 62* subjects (A = 50, B = 12). Temporal Cortex's RNAseq data from control subjects have *N = 70* subjects (A = 16, B = 34, C = 20). In RNAseq data from Cerebellum, individuals with Alzheimer's Disease have *N = 75* subjects (A = 18, B = 37 and C = 20); individuals with Progressive Supranuclear Palsy have *N = 62* subjects (A = 50, B = 12). Cerebellum's RNAseq data from control subjects have *N = 70* subjects (A = 16, B = 37, C = 17).

We used two animal models in this study: 5XFAD and TauD35. In the 5XFAD [36] model we analysed RNASeq data from hippocampus. We classified the animals into two groups, Alzheimer and Control, and subdivided them using the column "Age_Group" in three groups (4 M, 12 M, and 18 M, where M represents the month of the death), which can be found in the metadata from AMP-AD Knowledge portal (table 2). Thereby, in the Alzheimer's group we have 10 animals from subgroup 4 M, 9 from subgroup 12 M, and 16 from subgroup 18 M. In the control group, we have 10 animals from subgroup 4M, 10 animals from subgroup 12 M, and 20 from subgroup 18M. The TauD35 [37] model has RNAseq data from the hippocampus. Like the 5XFAD model, we classified the animals in Alzheimer and Control groups, subdividing them into 2 subgroups according to the month of the death of the animal. Alzheimer's groups have 9 animals, subdivided in 4 M (5 subjects) and 17 M (4 subjects); control groups have 11 animals, subdivided in 4 M (5 subjects) and 17 M (6 subjects).

To evaluate the transcription signature based on region we used RNAseq data from the Mount Sinai/JJ Peters VA Medical Center Brain Bank (MSBB–Mount Sinai NIH Neurobiobank) cohort (MSBB). This dataset contains data of four brain regions, although we decided to use just two: BA10 and BA36, where BA correspond to broadmann area. Simmilar to what we did in Mayo and mouse datasets we classified the data in Alzheimer and Control groups: BA10 have *N = 176 subjects* (Alzheimer = 105, Control = 71) and B36 have *N = 152* (Alzheimer = 88, Control = 64).

Realignment of human and animal models reads with Kallisto

We used the pipeline of Kallisto [38], a pseudoaligner tool to align all fastq files. The index used in the first step of the pipeline was GRCh38 cDNA release 94 (http://ftp.ensembl.org/pub/release-94/fasta/homo_sapiens/cdna) for the human data and the GRCm38 cDNA release 94 (http://ftp.ensembl.org/pub/release-94/fasta/mus_musculus/cdna) for both mouse animal models.

Differential gene expression analysis

To discover differentially expressed genes (DEGs) we used the DESeq2 R library [39] with the gene expression at transcription-level strategy; all variables and filters in the analyses using DESeq2 were equal to what we did in our previous work [14]. However, in this work we used the Age_Group variable from metadata into the design argument of the main *DESEq* function; thereby we could compare the affected groups (AD, PSP, and AD in animal models) with the control subjects based on the age of death.

For isoform switch/differential transcript usage (DTU) analysis we used the R library IsoformSwitchAnalyzeR [40]. All variables and filters in the analyses using this package were equal to what we did before in our previous work [14]. The only exception is that in this work we used differential isoform fraction (dIF) bigger than the module of 0.01, instead of 0.05. In addition, to the mouse animal models, we used as input the same cDNA release mentioned before in the Kallisto pseudoalignment pipeline (GRCM38 cDNA release 94) and the correspondent annotation (http://ftp.ensembl.org/pub/release-94/gtf/mus_musculus/Mus_musculus.GRCm38.94.chr_patch_hapl_scaff.gtf.gz).

Gene set enrichment analysis (GSEA) and Gene Ontology Network

For the gene ontology analysis, we used the R library gprofiler2 [41]. In the function *gost*, we set the parameters correction_method = “FDR” and significant=TRUE and a set of genes, divided into 3 groups: DEGs, gDTUs, and DEGs-gDTUs. We did this to all conditions and groups based on the age of death (A, B, and C for human data; 4M, 12M, 17M, and 18M for mouse data). The filters in this analysis were: false discovery rate (FDR) < 0.01; intersection size (intersection between gene set vs. a few genes in a term) > 3; and precision (intersection size divided by gene set) >0.03. We used the Gene Ontology (GO or by branch GO:MF, GO: BP, GO:CC) category to create the table with the results. For the construction of the gene ontology network, we used the results as Gene Matrix Transposed files (gmt): gmt files are archives with gene ontology terms and those genes enriched to the terms. To identify enriched terms sharing the same genes, we used the gmt file containing all gene ontology terms and the associated genes from the human species provided in gporfiler2’s website (gprofiler_full_hsapiens.name.gmt - https://biit.cs.ut.ee/gprofiler/static/gprofiler_hsapiens.name.zip).

We import this information in Cytoscape [42] and use the gmt expression files for each group, as mentioned before, and the gmt annotation file to construct the network of ontologies with the Enrinchmap plugin [43]. As result, we had a network of gene ontology terms where nodes correspond to gene ontology terms and edges to terms sharing the same genes. The node and edge tables from networks were exported and imported into R for a better visualization using the R library RedeR [44]. Only interactions with FDR < 0.05 and nodes with degree greater than 2 were shown. The name of a group of nodes was selected by the node with the higher degree.

Coexpression and module analysis

In the modules analysis, we used the R library CEMiTool [19], a package that unifies the discovery and the analysis of co-expression genes modules in a fully automatic manner. In this case modules are a set of genes with a similar expression. To know which and how many of it in each condition had, we used the main function *cemitool*. For the arguments, we used the normalized expression matrix of counts, metadata from every condition, *p_value* <0.1 (as suggested by the authors of the study), and *ora_pval < 0.01.* In this analysis, we did not subdivide subjects according to the age of death, just by condition, i.e, AD, PSP, and control. The final object from the analysis has some information about the modules found: which genes belong to the modules, Over Representation Analysis (ORA), Normalized Enrichment Score (NES), and Protein Protein Interaction (PPI). All these results were retrieved with the function *write_files()*. In ORA plots we showed just the GO terms with FDR<0.01. To know which modules are up or down-regulated between conditions, CEMiTool uses the fgsea [22] package. If this enrichment is significant, this information is summarized in the variable (NES), which is the enrichment score for a module in each class normalized by the number of genes in the module. Plots showing NES are only those modules with FDR<0.01.

The PPI networks in the figure 7 show networks with AD genes risk and PSP gene risk. The PPI of these figures were retrieved from the final object of Cemitool analysis and contains interactions between proteins. We decided to show only modules with AD or PSP risk genes.

Cell-ID

To evaluate the enrichment of module-specific gene set signatures in single-cell types, we used the R package Cell-ID [20]. This package allows a clustering-free multivariate statistical method for the robust extraction of per-cell gene signatures from single-cell RNASeq. In this work we used the single-cell signature from Leng's dataset [21], and performed MCA in scRNA-seq data from the entorhinal cortex of 3 healthy (Braak 0) individuals. Next, with CeII-ID we extracted and calculate the enrichment of per-cell gene signatures using as reference the list of genes from each module (S4 table) identified by CEMiTool. Statistical significance of this enrichment is calculated using a hypergeometric test and shown in function of -log10(pvalue).

References

1. __Montpetit V, Clapin DF, Guberman A. Substructure of 20 nm filaments of progressive supranuclear palsy. Acta Neuropathol (Berl). 1985;68(4):311–8.

2. __Kashyap G, Bapat D, Das D, Gowaikar R, Amritkar RE, Rangarajan G, et al. Synapse loss and progress of Alzheimer's disease -A network model. Sci Rep. 2019 Dec;9(1):6555.

3. __Wisniewski HM, Moretz RC, Lossinsky AS. Evidence for induction of localized amyloid deposits and neuritic plaques by an infectious agent. Ann Neurol. 1981 Dec;10(6):517–22.

4. __Boza-Serrano A, Yang Y, Paulus A, Deierborg T. Innate immune alterations are elicited in microglial cells before plaque deposition in the Alzheimer's disease mouse model 5xFAD. Sci Rep. 2018 Dec;8(1):1550.

5. __Allen M, Carrasquillo MM, Funk C, Heavner BD, Zou F, Younkin CS, et al. Human whole genome genotype and transcriptome data for Alzheimer's and other neurodegenerative diseases. Sci Data. 2016 Dec;3(1):160089.

6. __Drummond E, Wisniewski T. Alzheimer's disease: experimental models and reality. Acta Neuropathol (Berl). 2017 Feb;133(2):155–75.

7. __Castanho I, Murray TK, Hannon E, Jeffries A, Walker E, Laing E, et al. Transcriptional Signatures of Tau and Amyloid Neuropathology. Cell Rep. 2020 Feb;30(6):2040-2054.e5.

8. __Castillo-Carranza DL, Nilson AN, Van Skike CE, Jahrling JB, Patel K, Garach P, et al. Cerebral Microvascular Accumulation of Tau Oligomers in Alzheimer's Disease and Related Tauopathies. Aging Dis. 2017;8(3):257.

9. __Landel V, Baranger K, Virard I, Loriod B, Khrestchatisky M, Rivera S, et al. Temporal gene profiling of the 5XFAD transgenic mouse model highlights the importance of microglial activation in Alzheimer's disease. Mol Neurodegener. 2014;9(1):33.

10. _Matarin M, Salih DA, Yasvoina M, Cummings DM, Guelfi S, Liu W, et al. A Genome-wide Gene-Expression Analysis and Database in Transgenic Mice during Development of Amyloid or Tau Pathology. Cell Rep. 2015 Feb;10(4):633–44.

11. _Rothman SM, Tanis KQ, Gandhi P, Malkov V, Marcus J, Pearson M, et al. Human Alzheimer's disease gene expression signatures and immune profile in APP mouse models: a discrete transcriptomic view of Aβ plaque pathology. J Neuroinflammation. 2018 Dec;15(1):256.

12. _Swarup V, Hinz FI, Rexach JE, Noguchi K, Toyoshiba H, Oda A, et al. Identification of evolutionarily conserved gene networks mediating neurodegenerative dementia. Nat Med. 2019 Jan;25(1):152–64.

13. _Wan Y-W, Al-Ouran R, Mangleburg CG, Perumal TM, Lee TV, Allison K, et al. Meta-Analysis of the Alzheimer's Disease Human Brain Transcriptome and Functional Dissection in Mouse Models. Cell Rep. 2020 Jul;32(2):107908.

14. _Marques-Coelho D, Iohan L da CC, Melo de Farias AR, Flaig A, Lambert J-C, Costa MR. Differential transcript usage unravels gene expression alterations in Alzheimer's disease human brains. Npj Aging Mech Dis. 2021 Dec;7(1):2.

15. _Mungas D, Reed BR, Ellis WG, Jagust WJ. The Effects of Age on Rate of Progression of Alzheimer Disease and Dementia With Associated Cerebrovascular Disease. Arch Neurol. 2001 Aug 1;58(8):1243.

16. _Arena JE, Weigand SD, Whitwell JL, Hassan A, Eggers SD, Höglinger GU, et al. Progressive supranuclear palsy: progression and survival. J Neurol. 2016 Feb;263(2):380–9.

17. _Rajput A, Rajput AH. Progressive Supranuclear Palsy: Clinical Features, Pathophysiology and Management. Drugs Aging. 2001;18(12):913–25.

18. _Chung DC, Roemer S, Petrucelli L, Dickson DW. Cellular and pathological heterogeneity of primary tauopathies. Mol Neurodegener. 2021 Dec;16(1):57.

19. _Russo PST, Ferreira GR, Cardozo LE, Bürger MC, Arias-Carrasco R, Maruyama SR, et al. CEMiTool: a Bioconductor package for performing comprehensive modular co-expression analyses. BMC Bioinformatics. 2018 Dec;19(1):56.

20. _Akira C, Loredana M, Emmanuelle S, Antonio R. Cell-ID: gene signature extraction and cell identity recognition at individual cell level [Internet]. Bioinformatics; 2020 Jul [cited 2021 Sep 15]. Available from: http://biorxiv.org/lookup/doi/10.1101/2020.07.23.215525

21. _Leng K, Li E, Eser R, Piergies A, Sit R, Tan M, et al. Molecular characterization of selectively vulnerable neurons in Alzheimer's disease. Nat Neurosci. 2021 Feb;24(2):276–87.

22. _Korotkevich G, Sukhov V, Budin N, Shpak B, Artyomov MN, Sergushichev A. Fast gene set enrichment analysis [Internet]. Bioinformatics; 2016 Jun [cited 2021 Sep 15]. Available from: http://biorxiv.org/lookup/doi/10.1101/060012

23. _Wang M, Beckmann ND, Roussos P, Wang E, Zhou X, Wang Q, et al. The Mount Sinai cohort of large-scale genomic, transcriptomic and proteomic data in Alzheimer's disease. Sci Data. 2018 Dec;5(1):180185.

24. _Braak H, Braak E. Neuropathological stageing of Alzheimer-related changes. Acta Neuropathol (Berl). 1991;82(4):239–59.

25. _Höglinger GU, Melhem NM, Dickson DW, Sleiman PMA, Wang L-S, Klei L, et al. Identification of common variants influencing risk of the tauopathy progressive supranuclear palsy. Nat Genet. 2011 Jul;43(7):699–705.

26. _Lambert J-C, Ibrahim-Verbaas CA, Harold D, Naj AC, Sims R, Bellenguez C, et al. Meta-analysis of 74,046 individuals identifies 11 new susceptibility loci for Alzheimer's disease. Nat Genet. 2013 Dec;45(12):1452–8.

27. _Kunkle BW, Grenier-Boley B, Sims R, Bis JC, Damotte V, Naj AC, et al. Genetic meta-analysis of diagnosed Alzheimer's disease identifies new risk loci and implicates Aβ, tau, immunity and lipid processing. Nat Genet. 2019 Mar;51(3):414–30.

28. _Armstrong RA, Cairns NJ. Spatial patterns of the tau pathology in progressive supranuclear palsy. Neurol Sci. 2013 Mar;34(3):337–44.

29. _Raj T, Li YI, Wong G, Humphrey J, Wang M, Ramdhani S, et al. Integrative transcriptome analyses of the aging brain implicate altered splicing in Alzheimer's disease susceptibility. Nat Genet. 2018 Nov;50(11):1584–92.

30. _Allen M, Wang X, Burgess JD, Watzlawik J, Serie DJ, Younkin CS, et al. Conserved brain myelination networks are altered in Alzheimer's and other neurodegenerative diseases. Alzheimers Dement. 2018 Mar;14(3):352–66.

31. _Togo T, Dickson DW. Tau accumulation in astrocytes in progressive supranuclear palsy is a degenerative rather than a reactive process. Acta Neuropathol (Berl). 2002 Oct;104(4):398–402.

32. _Tsai AP, Lin PB-C, Dong C, Moutinho M, Casali BT, Liu Y, et al. INPP5D expression is associated with risk for Alzheimer's disease and induced by plaque-associated microglia. Neurobiol Dis. 2021 Jun;153:105303.

33. _Zhou Y, Ulland TK, Colonna M. TREM2-Dependent Effects on Microglia in Alzheimer's Disease. Front Aging Neurosci. 2018 Jul 9;10:202.

34. _Moreau-Fauvarque C, Kumanogoh A, Camand E, Jaillard C, Barbin G, Boquet I, et al. The Transmembrane Semaphorin Sema4D/CD100, an Inhibitor of Axonal Growth, Is Expressed on Oligodendrocytes and Upregulated after CNS Lesion. J Neurosci. 2003 Oct 8;23(27):9229–39.

35. _Schäfer I, Müller C, Luhmann HJ, White R. MOBP levels are regulated by Fyn kinase and affect the morphological differentiation of oligodendrocytes. J Cell Sci. 2016 Jan 1;jcs.172148.

36. _Oakley H, Cole SL, Logan S, Maus E, Shao P, Craft J, et al. Intraneuronal beta-Amyloid Aggregates, Neurodegeneration, and Neuron Loss in Transgenic Mice with Five Familial Alzheimer's Disease Mutations: Potential Factors in Amyloid Plaque Formation. J Neurosci. 2006 Oct 4;26(40):10129–40.

37. _Terwel D, Lasrado R, Snauwaert J, Vandeweert E, Van Haesendonck C, Borghgraef P, et al. Changed Conformation of Mutant Tau-P301L Underlies the Moribund Tauopathy, Absent in Progressive, Nonlethal Axonopathy of Tau-4R/2N Transgenic Mice. J Biol Chem. 2005 Feb;280(5):3963–73.

38. _Bray NL, Pimentel H, Melsted P, Pachter L. Near-optimal probabilistic RNA-seq quantification. Nat Biotechnol. 2016 May;34(5):525–7.

39. _Love MI, Huber W, Anders S. Moderated estimation of fold change and dispersion for RNA-seq data with DESeq2. Genome Biol. 2014 Dec;15(12):550.

40. _Vitting-Seerup K, Sandelin A. IsoformSwitchAnalyzeR: analysis of changes in genome-wide patterns of alternative splicing and its functional consequences. Berger B, editor. Bioinformatics. 2019 Nov 1;35(21):4469–71.

41. _Raudvere U, Kolberg L, Kuzmin I, Arak T, Adler P, Peterson H, et al. g:Profiler: a web server for functional enrichment analysis and conversions of gene lists (2019 update). Nucleic Acids Res. 2019 Jul 2;47(W1):W191–8.

42. _Shannon P. Cytoscape: A Software Environment for Integrated Models of Biomolecular Interaction Networks. Genome Res. 2003 Nov 1;13(11):2498–504.

43. _Merico D, Isserlin R, Stueker O, Emili A, Bader GD. Enrichment Map: A Network-Based Method for Gene-Set Enrichment Visualization and Interpretation. Ravasi T, editor. PLoS ONE. 2010 Nov 15;5(11):e13984.

44. Castro MA, Wang X, Fletcher MN, Meyer KB, Markowetz F. RedeR: R/Bioconductor package for representing modular structures, nested networks and multiple levels of hierarchical associations. Genome Biol. 2012;13(4):R29

Acknowledgments

The results published here are in whole or in part based on data obtained from the AMP-AD Knowledge Portal (https://adknowledgeportal.synapse.org/). Study data were provided by the following sources: The Mayo Clinic Alzheimer's Disease Genetic Studies, led by Dr. Nilufer Taner and Dr. Steven G. Younkin, Mayo Clinic, Jacksonville, FL using samples from the Mayo Clinic Study of Aging, the Mayo Clinic Alzheimer's Disease Research Center, and the Mayo Clinic Brain Bank. Data collection was supported through funding by NIA grants P50 AG016574, R01 AG032990, U01 AG046139, R01 AG018023, U01 AG006576, U01 AG006786, R01 AG025711, R01 AG017216, R01 AG003949, NINDS grant R01 NS080820, CurePSP Foundation, and support from Mayo Foundation. Study data includes samples collected through the Sun Health Research Institute Brain and Body Donation Program of Sun City, Arizona. The Brain and Body Donation Program is supported by the National Institute of Neurological Disorders and Stroke (U24 NS072026 National Brain and Tissue Resource for Parkinson's Disease and Related Disorders), the National Institute on Aging (P30 AG19610 Arizona Alzheimer's Disease Core Center), the Arizona Department of Health Services (contract 211002, Arizona Alzheimer's Research Center), the Arizona Biomedical Research Commission (contracts 4001, 0011, 05-901 and 1001 to the Arizona Parkinson's Disease Consortium) and the Michael J. Fox Foundation for Parkinson's Research. Study data were also generated from postmortem brain tissue collected through the Mount Sinai VA Medical Center Brain Bank and were provided by Dr. Eric Schadt from Mount Sinai School of Medicine. We also thank GSK and Company scientists for generating the TauD35 RNASeq data and providing us access to them. 5XFAD mice are provided through the IU/JAX/UCI MODEL-AD Center, established with funding from The National Institute on Aging (U54 AG054345-01 and AG054349). Aging studies are also supported by the Nathan Shock Center of Excellence in the Basic Biology of Aging (NIH P30 AG0380770).

This work was co-funded by the European Union under the European Regional Development Fund (ERDF) and by the Hauts de France Regional Council (contract n°18006176), the MEL (contract_2016_ESR_05), and the French State (contract n°2018-3-CTRL_IPL_Phase2) to MRC. This work was also funded by the Lille Métropole Communauté Urbaine and the French government’s LABEX DISTALZ program (Development of innovative strategies for a transdisciplinary approach to Alzheimer’s disease) to JCL. LICC is supported by the Coordenação de Aperfeiçoamento de Pessoal de Nível Superior (CAPES) scholarship.

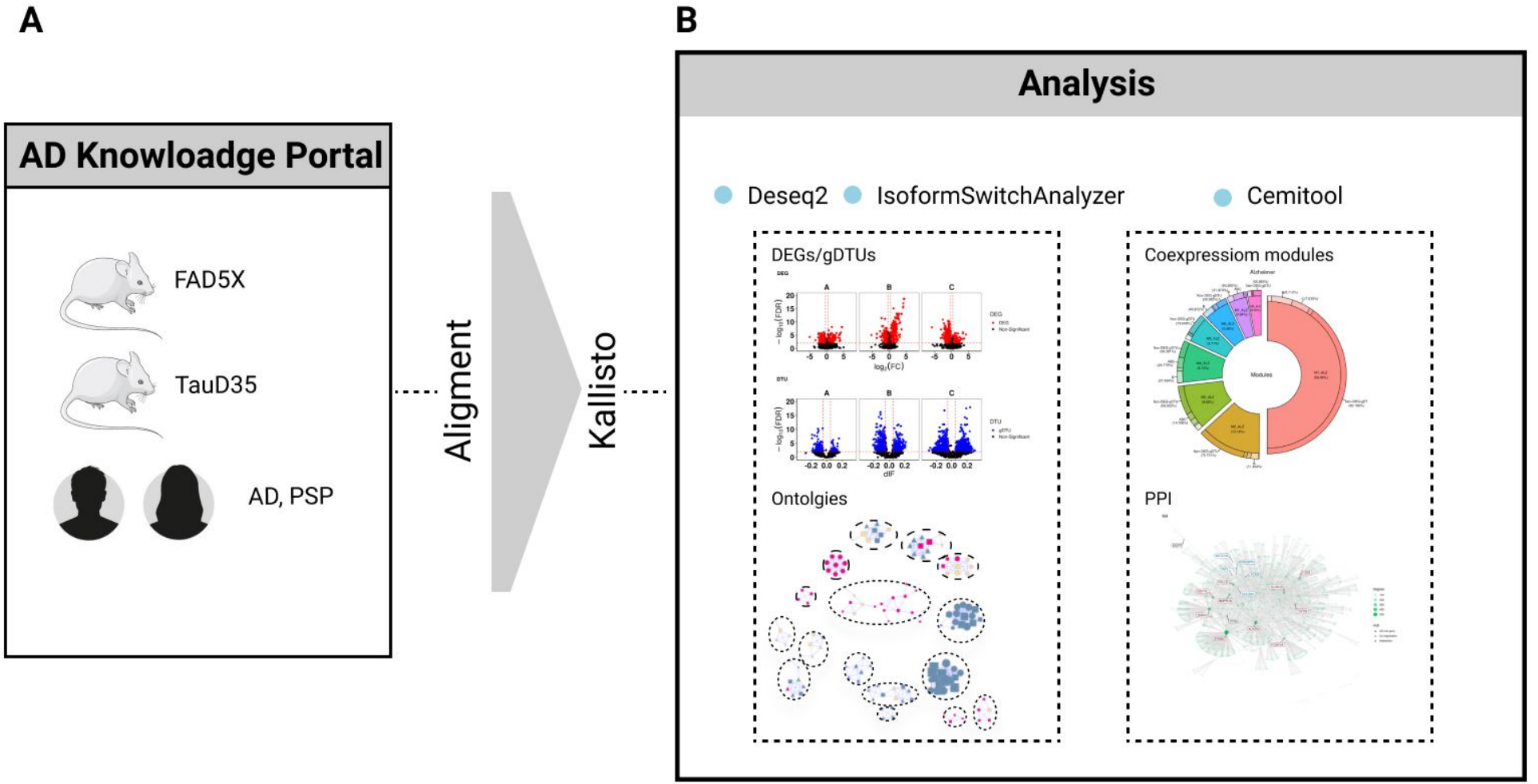

Figure 1 - Schematic summay of methodolody. A Human (AD, PSP) and mouse (5XFAD, TauD35) RNA-seq data were obtained from the AD Knowloadge Portal and grouped acccording to the age of death. Next, RNAseq data was pseudo-aligned using Kallisto. **B** Analyses were performed using three R packages: DESeq2, IsoformSwitchAnalyzer, gprofiler2 and CEMiTool.

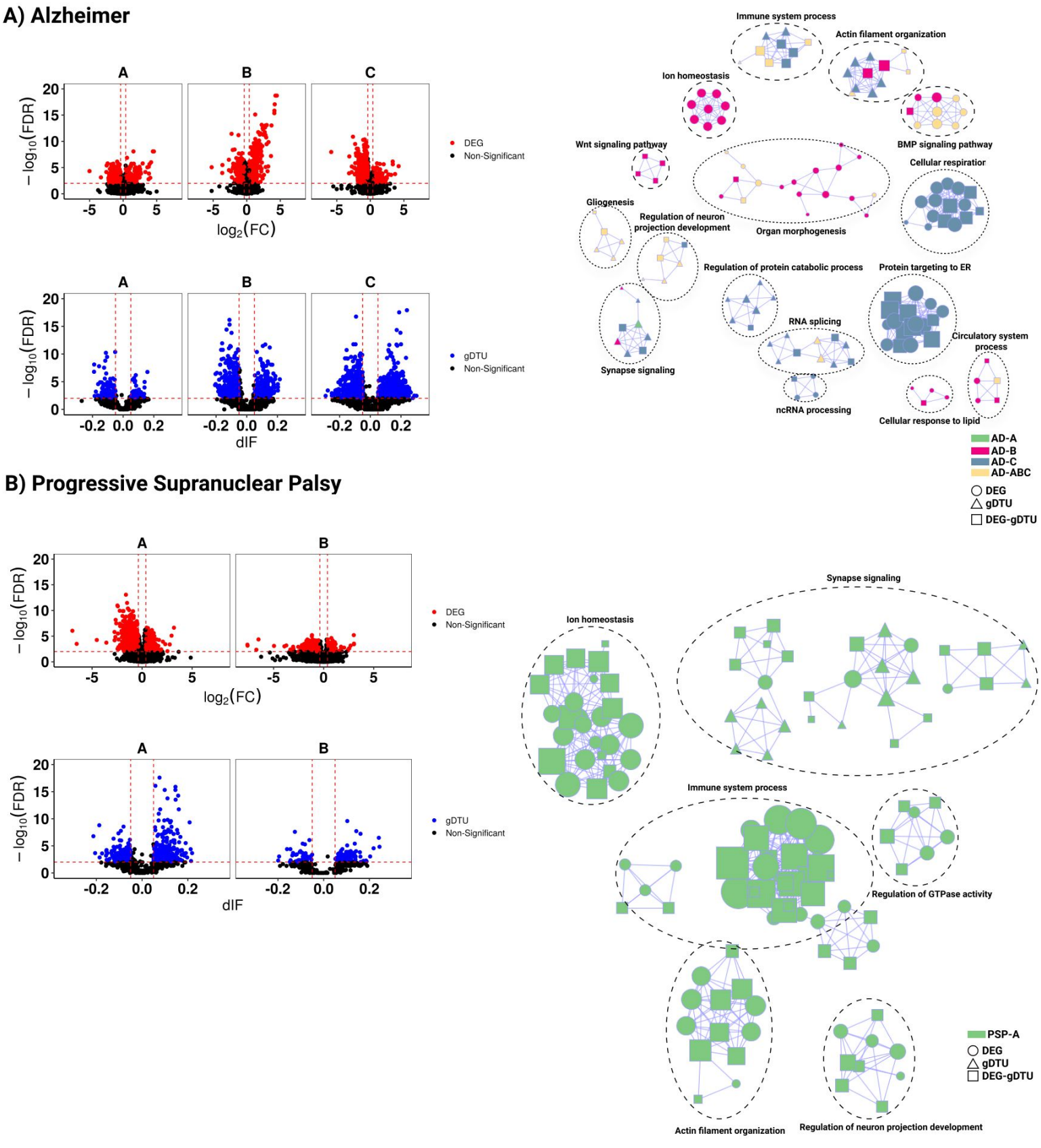

Figure 2 - Gene expression alterations in the temporal cortex of AD and PSP patients. A Volcano plots showing differentetially expressed genes (DEGs, red dots; FC > 1.3 and FDR < 0.01), genes with differential transcript usage (gDTU, blue dots; Differential isoform fraction (dIF) and FDR < 0.01) and a network of gene ontologies significantly enriched in AD. **B** Same for PSP. AD (Alzheimer's disease), PSP (Progressive Supranuclear Palsy), A (age of death between 70-80 years old), B (age of death between 81-89 years old), C (age of death equal or superior to 90 years old), FDR (False Discovery Rate).

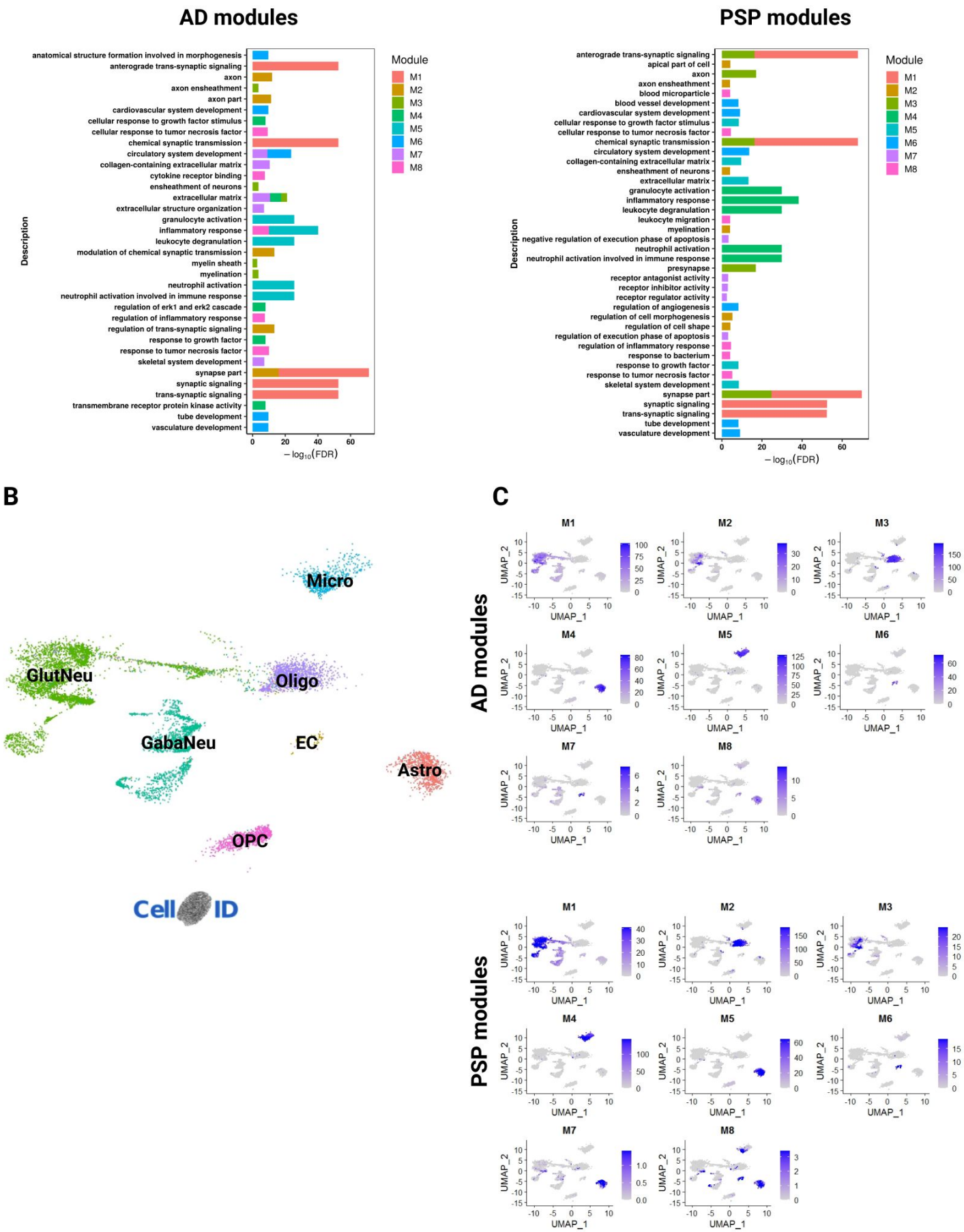

Figure 3 - Gene coexpression modules are associated with cell-type especific processes. **A** ORA (Over Representation Analysis) for modules identified in AD and PSP in temporal cortex RNA-seq data. **B** Dimension plot showing major cell types identified in a scRNA-seq dataset generated from the adult human brain (Leng et al., 2021). **C** Feature plots showing the enrichment of genes identified in different modules. Scale indicates -log10(Pvalue) for the hypergeometric test used in CellID. Astro (Astrocyte), EC (Endothelial cell), GabaNeu (Gabaergic Neuron), GlutNeu (Glutamatergic Neuron), Micro (Microglia), Oligo (Oligodendrocyte) , OPC (Oligodendrocyte Precursor Cell). In ORA, only ontologies with FDR < 0.01 are shown.

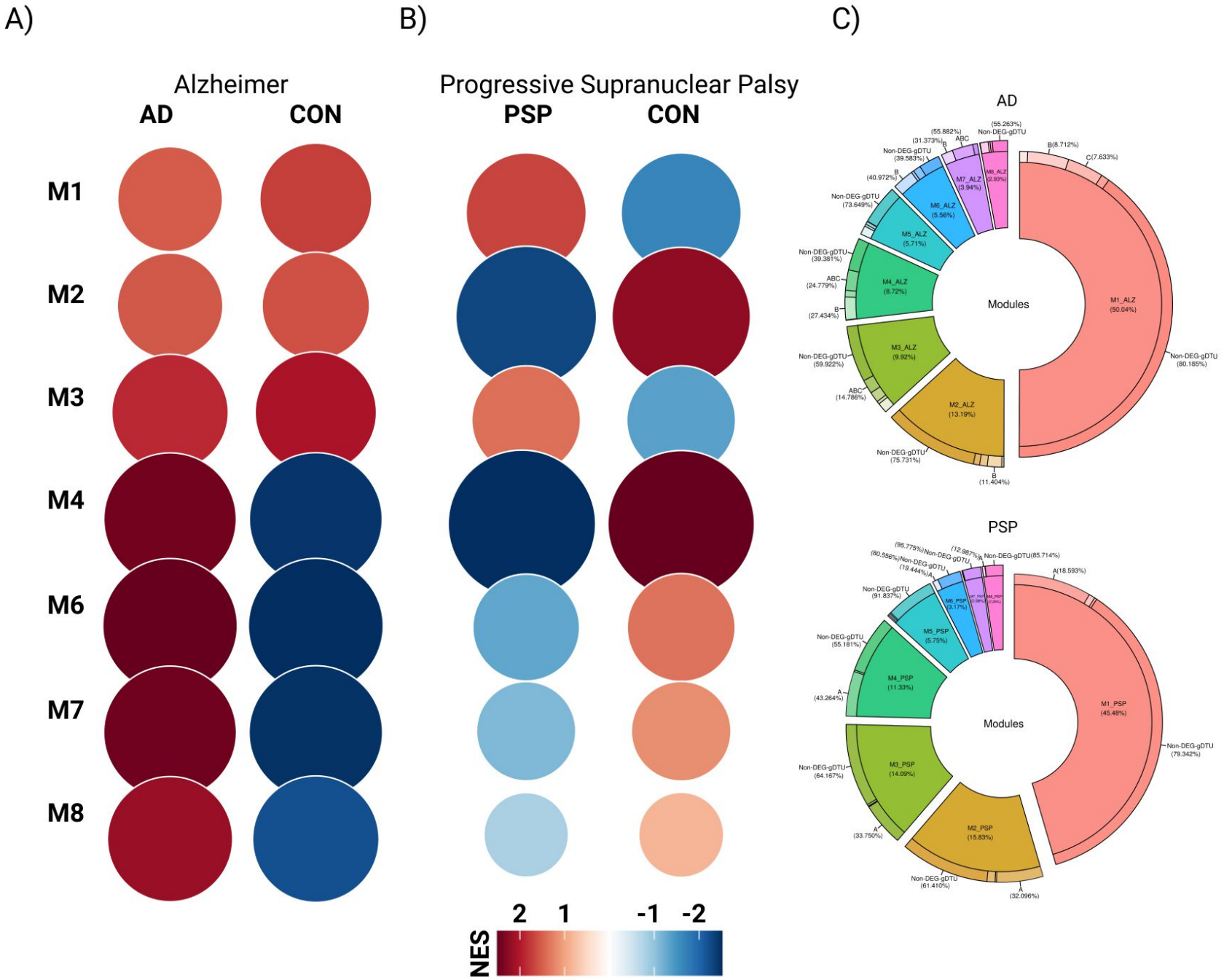

Figure 4 - Immune and synaptic module have differente enrichment in AD and PSP. A NES for modules found in AD temporal cortex data. **B** NES for modules found in PSP temporal cortex data. **C** Proportion of genes in each module for AD and PSP. NES (Normalised Enrichment Score).

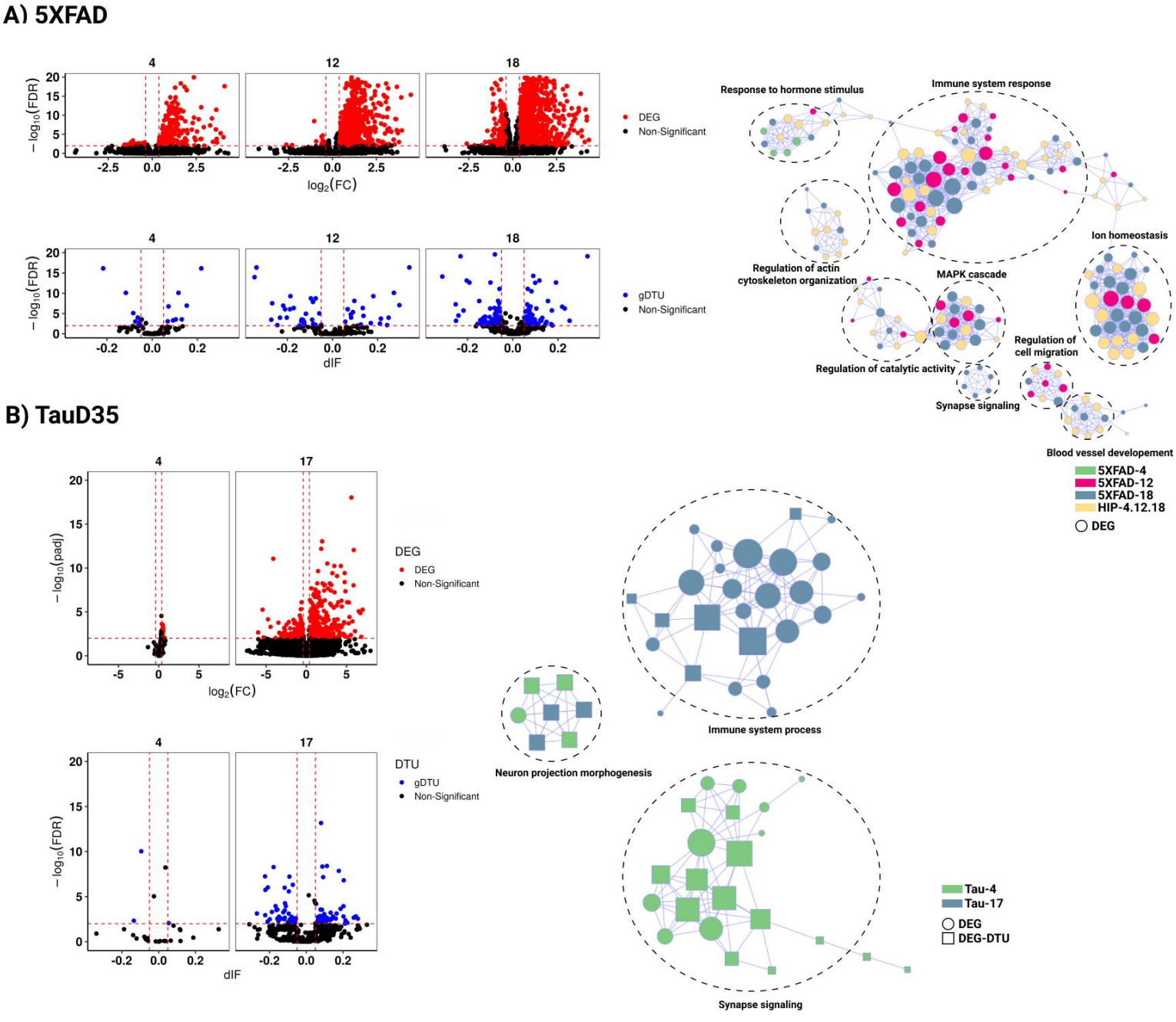

Figure 5 - Gene expression alterations in animal models of amyloidopathy and tauopathy. A Volcano plots showing differentetially expressed genes (DEGs, red dots; FC > 1.3 and FDR < 0.01), genes with differential transcript usage (gDTU, blue dots; Differential isoform fraction (dIF) and FDR < 0.01) and a network of ontologies for the 5XFAD mouse model data. **B** Same for TauD35 mouse model data.
4 (four months), 12 (twelve months), 17 (seventeen months), 18 (eighteen months), FDR (False Discovery Rate).

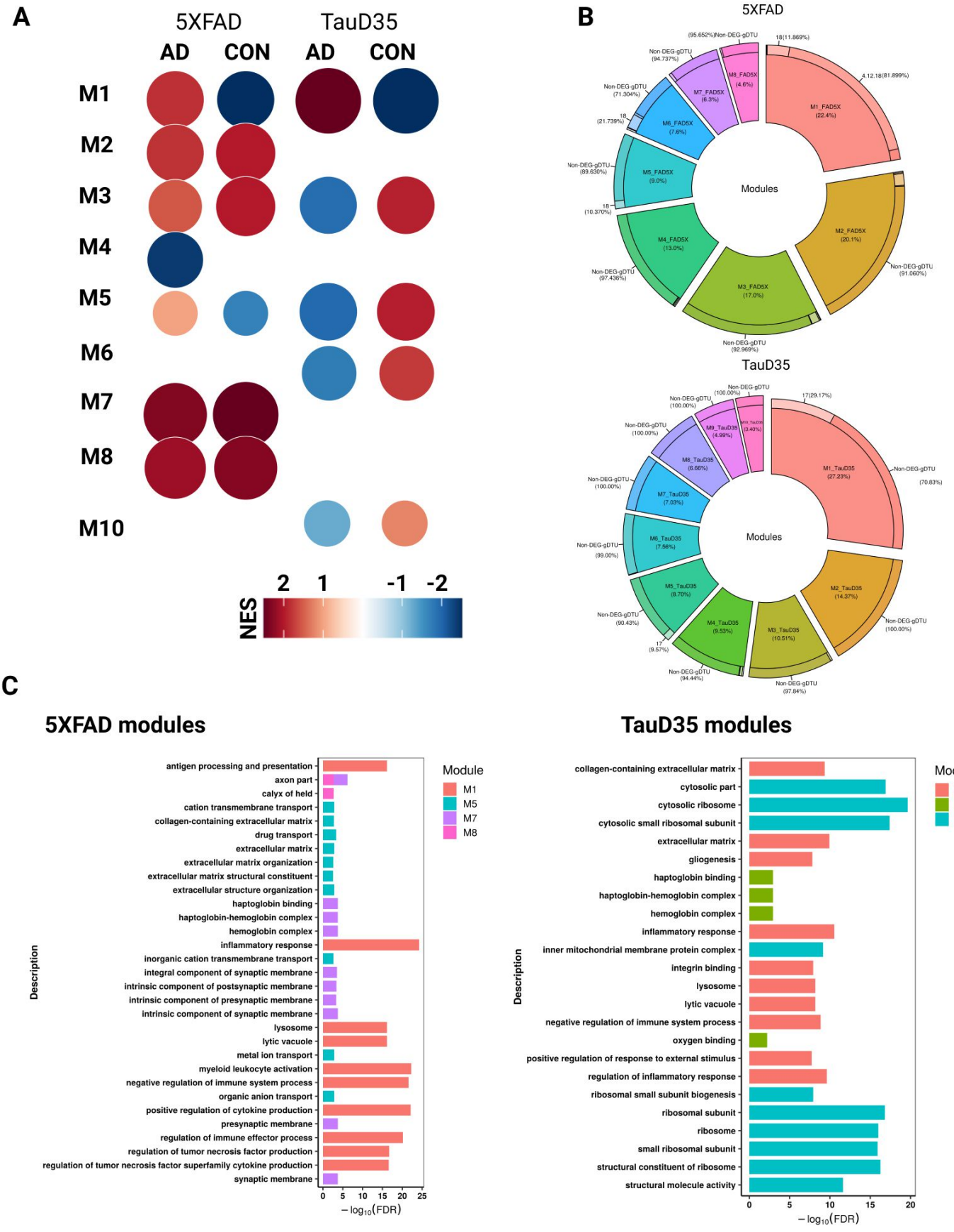

Figure 6 - Immune and synaptic modules have differente enrichment in 5XFAD and TauD35. A NES for modules found in 5XFAD and TauD35. **B** Proportion of genes in each module for 5XFAD and TauD35. **C** ORA (Over Representative analysis) form modules found in 5XFAD and TauD35
NES (Normalised Enrichment Score). In ORA, only ontologies with FDR < 0.01 are shown.

A) Alzheimer

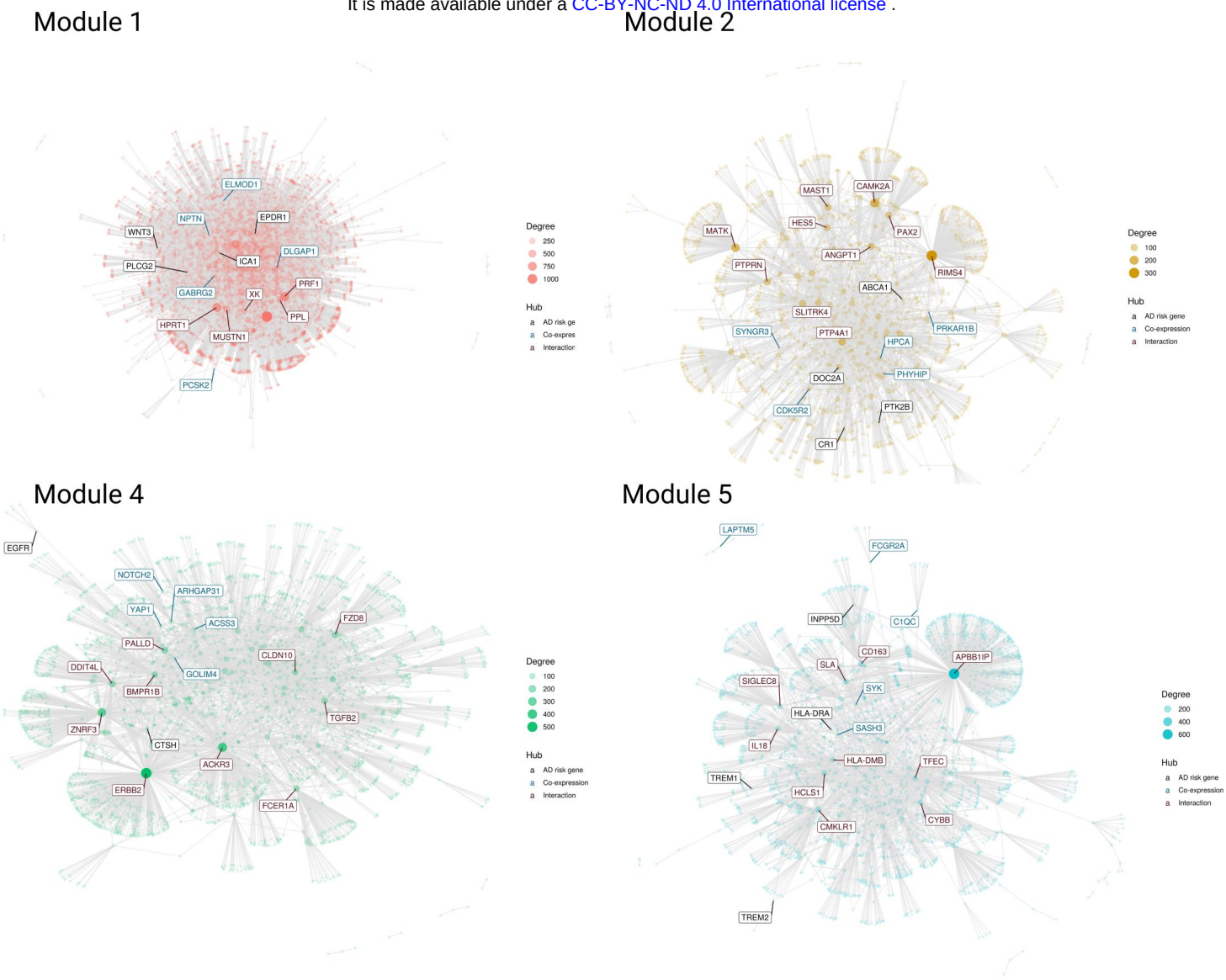

B) Progressive Supranuclear Palsy

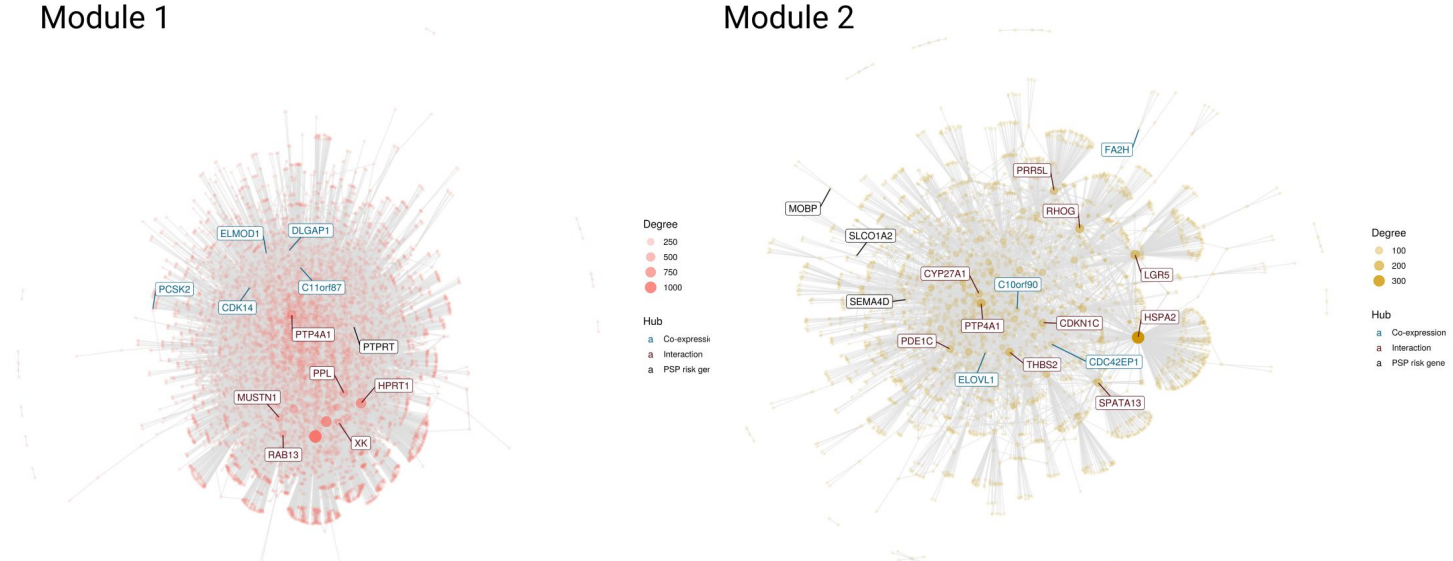

Figure 7 - AD and PSP risk genes are present in some modules. A AD risk genes found in the PPI of modules. **B** PSP risk genes found im PPI of modules. AD and PSP risk genes are labeled in black. Genes labeled in blue are part of modules and genes labeled in red are derived of interaction files from CEMiTool's package, and represent genes with higher degree in the PPI.

A) DEGs per Age

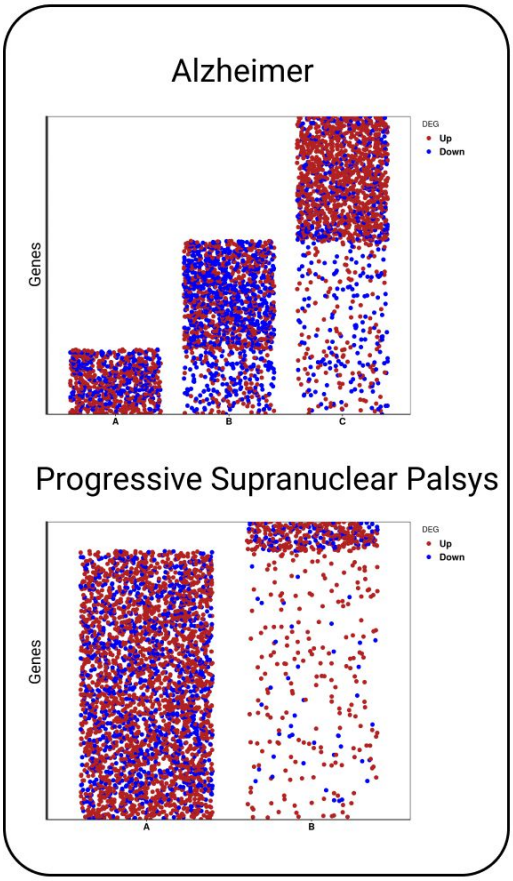

C) DEGs per Age

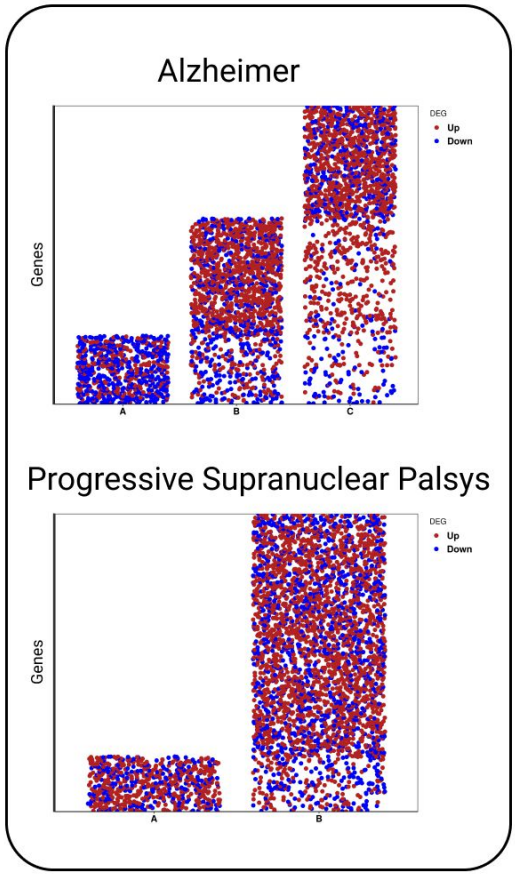

B) Intercept - Temporal Cortex

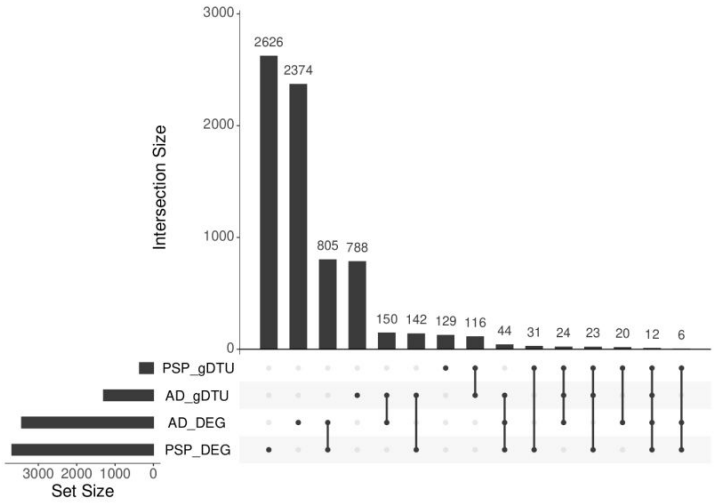

D) Intercept - Cerebellum

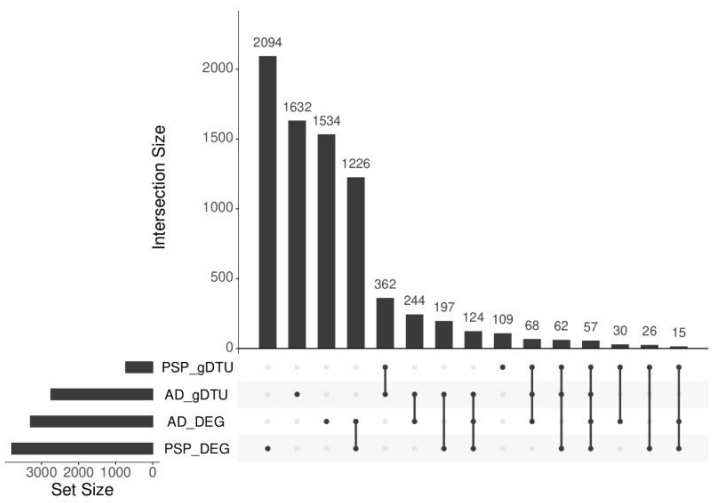

Suplementary figure 1 - Unique gene expression alterations in temporal cortex and cerebellum at different ages. A DEGs from temporal cortex data of AD and PSP. **B** Intercept graphic of DEGs and gDTUS between AD and PSP genes from temporal cortex data. Conected lines represent data with same genes . **C** DEGs from cerebellum data of AD and PSP. **D** Intercept graphic of DEGs and gDTUS between AD and PSP genes from cerebellum data. Conected lines represent data with same genes.

Up (genes with higher expression when comparared to control individuals), Down (genes with lower expression when comparared to control individuals).

A) Alzheimer

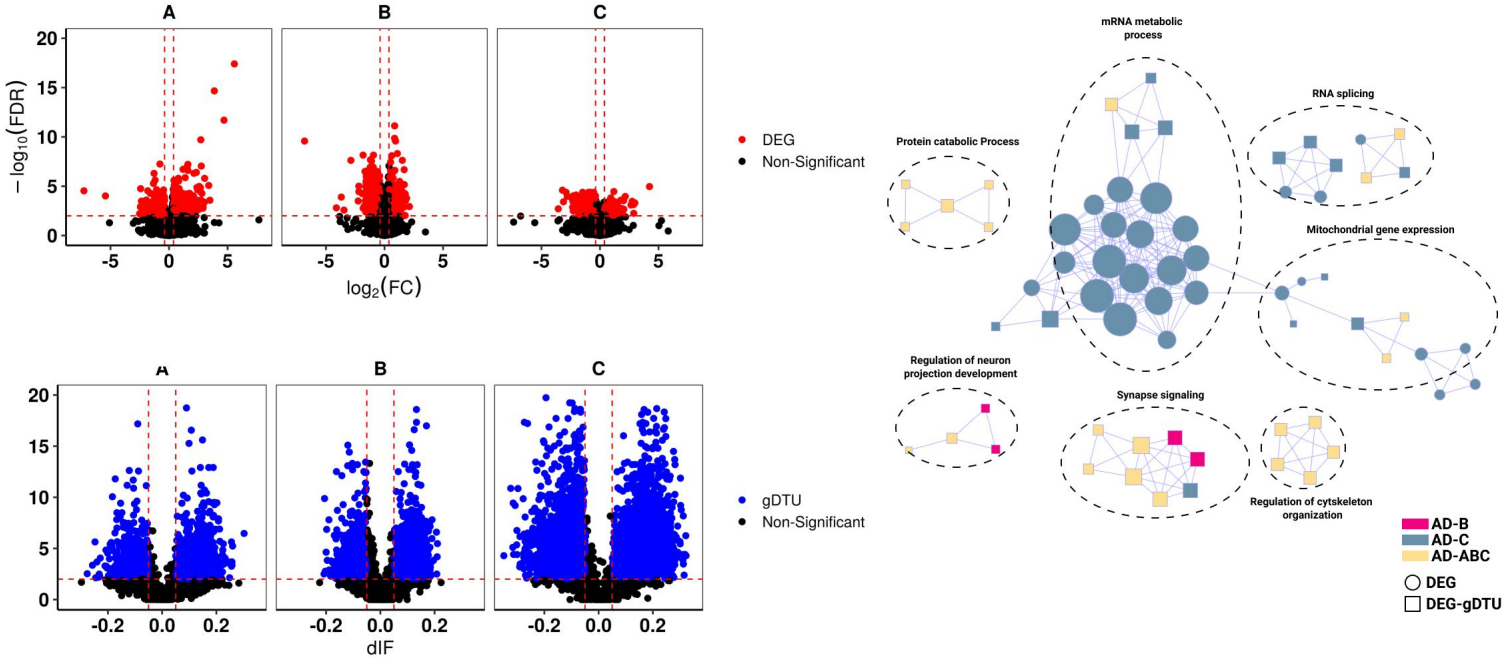

B) Progressive Supranuclear Palsy

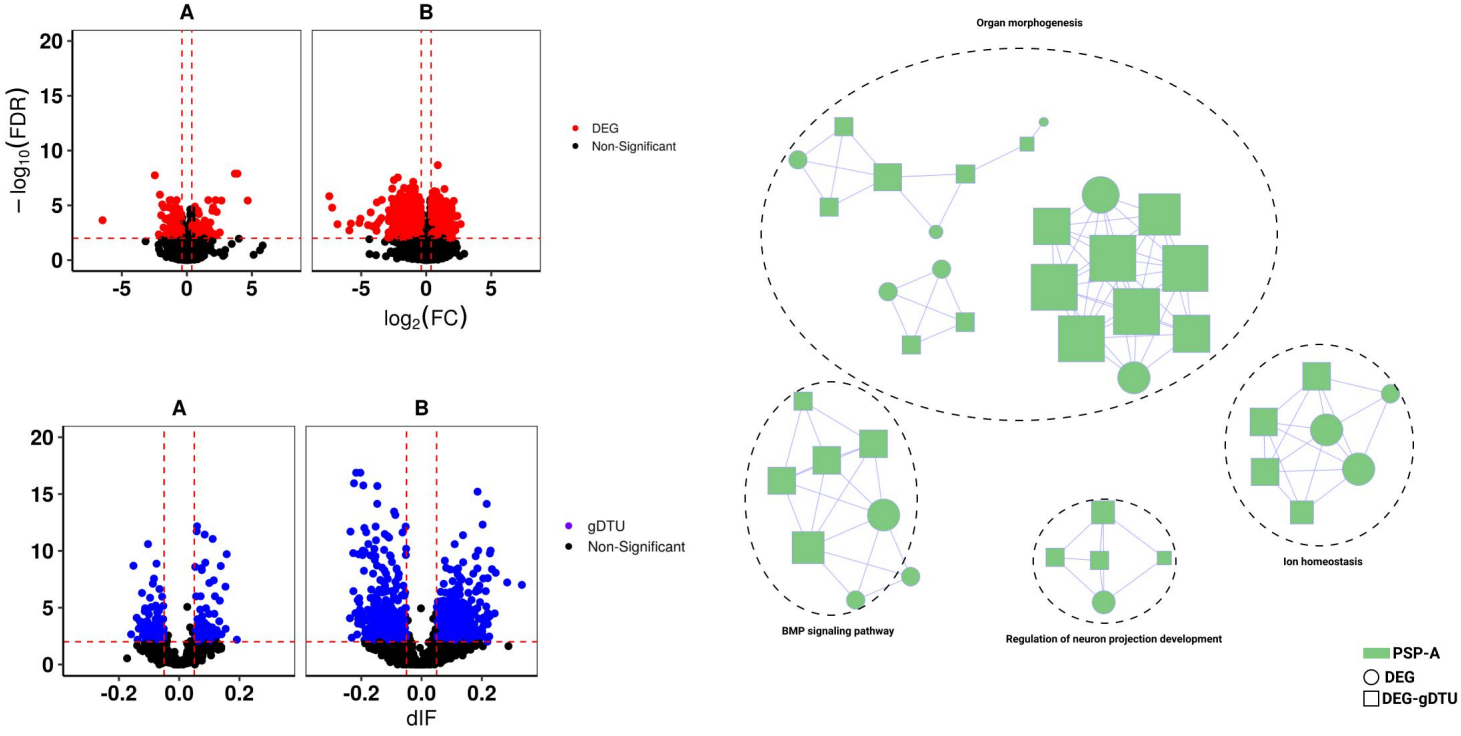

Supmentary figure 2 - Gene expression alterations in the cerebellum of AD and PSP patients. A Volcano plots showing differentetially expressed genes (DEGs, red dots; FC > 1.3 and FDR < 0.01), genes with differential transcript usage (gDTU, blue dots; Differential isoform fraction (dIF) and FDR < 0.01) and a network of ontologies for Alzheimer in cerebellum. **B** Same for PSP.
AD (Alzheimer), PSP (Progressive Supranuclear Palsy), A (age of death between 70-80 years old), B (age of death between 81-89 years old), C (age of death equal or superior to 90 years old), FDR (False Discovery Rate).

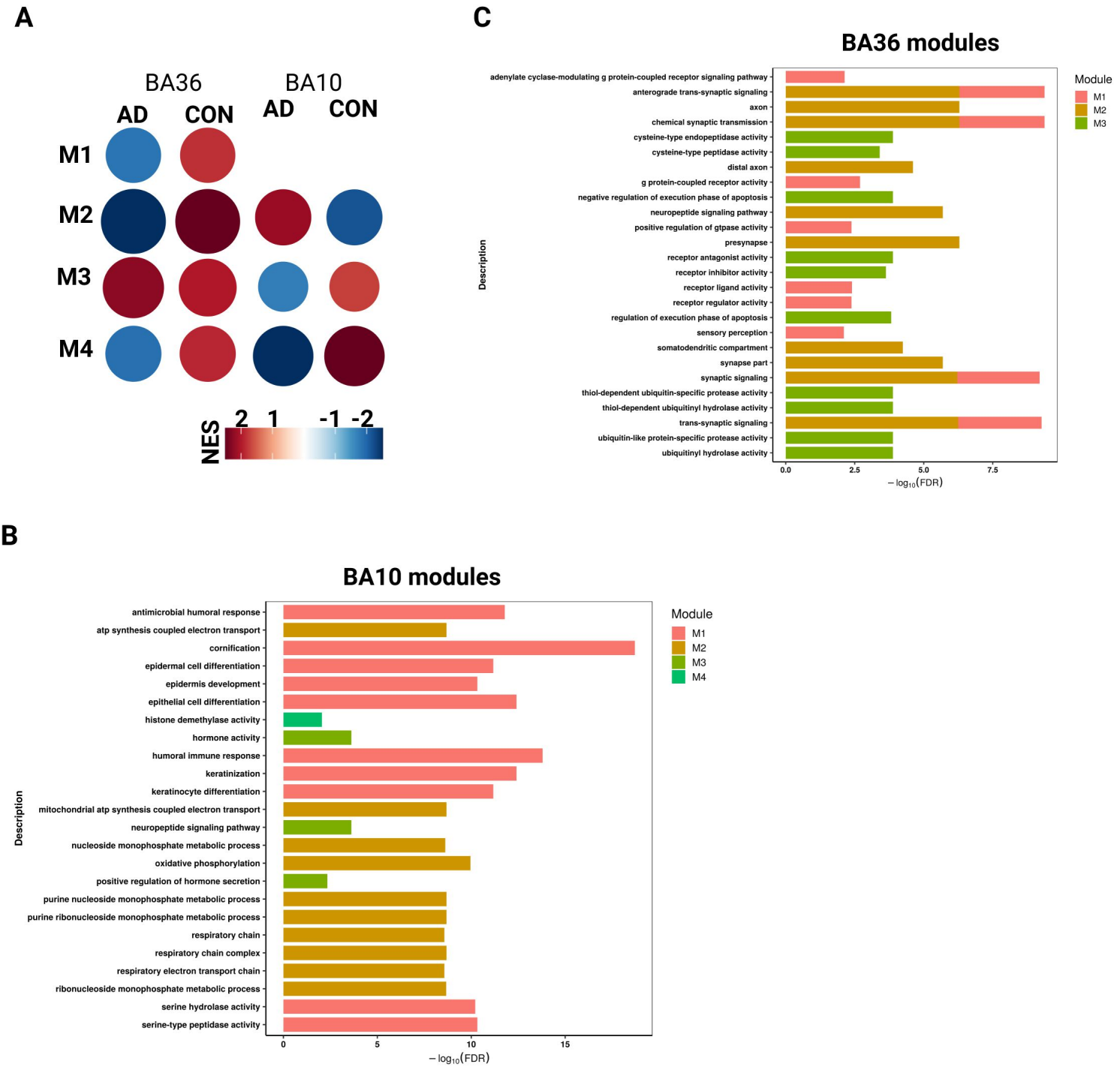

Suplementary figure 3 - Gene expression alterations associated with immune system and synaposes follow pathology progression in AD brains. A NES for modules found in BA36 and BA10 areas. **B** ORA (Over Representative Analysis) of BA10 modules. **C** ORA (Over Representative Analysis) of BA36 modules.
BA10 (Broadmann area 10), BA36 (Broadmann area 36). In ORA, only ontologies with FDR < 0.01 are shown.

A) DEGs per Age

B) DEGs per Age

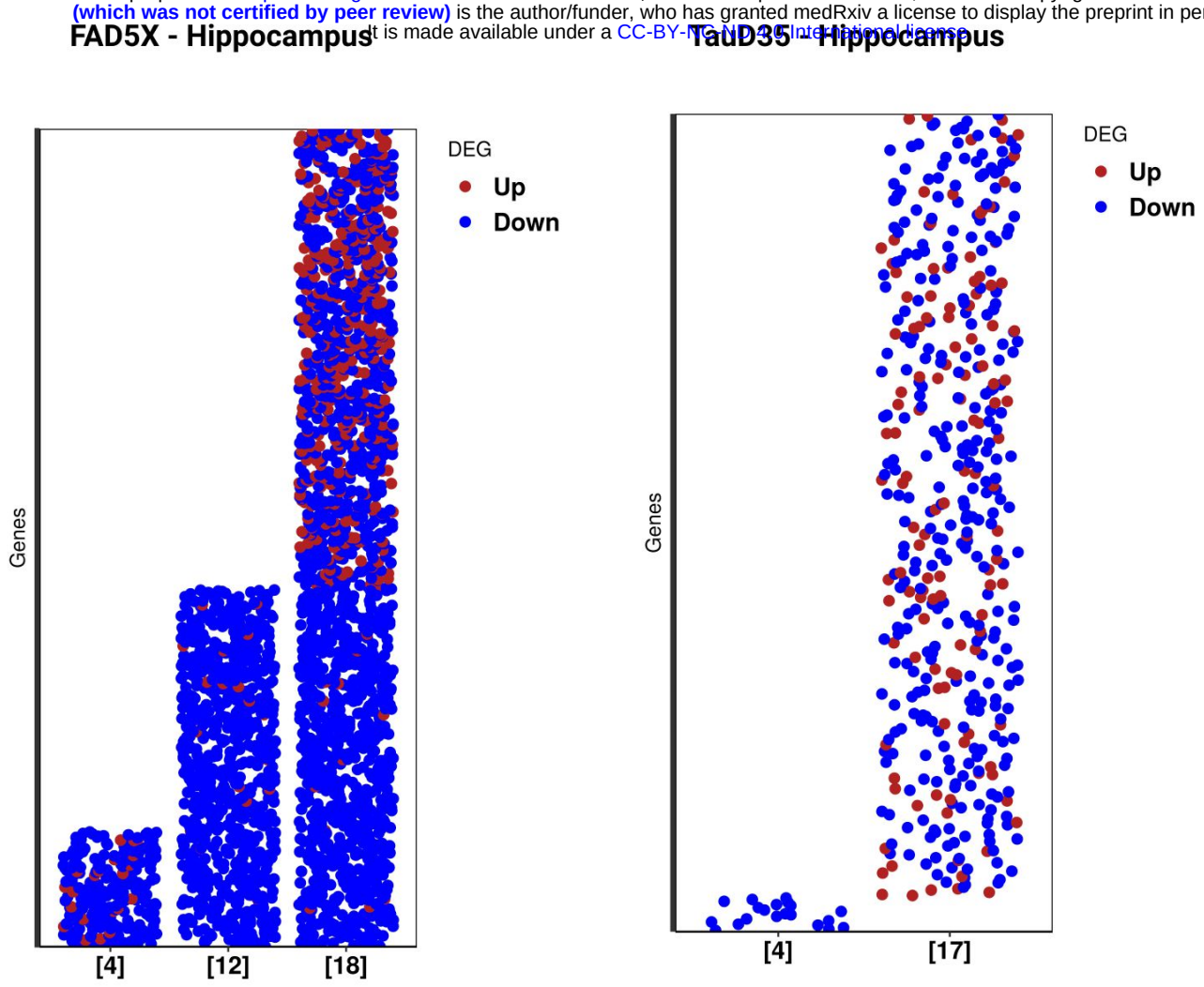

C) Intercept - FAD5X | TauD35

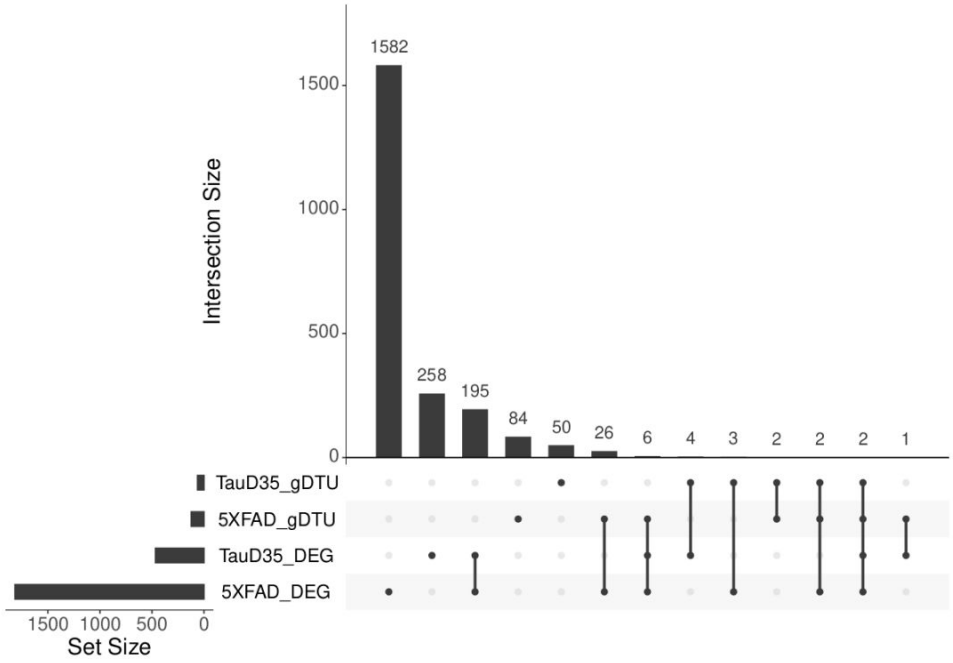

Suplementary figure 4 - Isoform switches (gDTUS) are rare in the brains of AD animal models. A DEGs 5XFAD data. **B** DEGS from TauD35 data C Intercept graphic of DEGs and gDTUS between 5XFAD and TauD35 animal models. Conected lines represent data with same genes.
Up (genes with higher expression when comparared to control animals), Down (genes with lower expression when comparared to control animals).

Table 1. Summary of clinical, demographich, and technical variables of samples of temporal human TCX data

Temporal Cortex

Information Human

Age_Group	Sex	n	AOD	Braak	RIN	PMI
AD						
A	male	8	76.75 (± 2.25)	5.31 (± 0.46)	8.47 (± 0.38)	9 (± 8.72)
A	female	10	76 (± 3.13)	5.6 (± 0.52)	8.55 (± 0.53)	5.29 (± 4.82)
B	female	23	85.13 (± 2.88)	5.52 (± 0.55)	8.69 (± 0.65)	6.07 (± 4.57)
B	male	14	85.21 (± 2.08)	5.39 (± 0.63)	8.64 (± 0.65)	8.09 (± 5.49)
C	female	13	90+	5.54 (± 0.56)	8.31 (± 0.34)	8.38 (± 8.93)
C	male	7	90+	5.29 (± 0.49)	8.63 (± 0.45)	8.25 (± 5.25)
PSP						
A	female	21	75.48 (± 3.76)	2.1 (± 0.89)	8.45 (± 0.47)	7.78 (± 6.22)
A	male	29	75.31 (± 3.06)	2.14 (± 0.92)	8.43 (± 0.53)	9.27 (± 7.52)
B	female	3	82.33 (± 2.31)	1.17 (± 1.26)	8.23 (± 0.25)	11.33 (± 2.08)
B	male	9	84.11 (± 2.37)	2.39 (± 0.99)	8.69 (± 0.53)	3.5 (± 0.71)
Control						
A	female	3	76.67 (± 2.08)	-	7.77 (± 1.54)	3 (± 1.41)
A	male	13	76 (± 2.97)	-	7.25 (± 0.95)	2.6 (± 0.84)
B	female	19	86.47 (± 2.04)	-	7.93 (± 0.81)	4.5 (± 3.14)
B	male	15	84.87 (± 2.9)	-	7.68 (± 0.83)	5.71 (± 5.55)
C	female	12	90+	-	7.06 (± 0.92)	13.78 (± 10.96)
C	male	8	90+	2.31 (± 1)	8.28 (± 1.51)	11.29 (± 10.21)

AOD = Age of Death, **n** = number of samples, **RIN** = RNA integrity number, **PMI** = Postmortem interval (in hours).
ALZ = Alzheimer Disease.
PSP = Progressive Supranuclear Palsy.
Values are mean ± SD.

Table 2. Summary of clinical, demographich, and technical variables of samples of human CER data

Cerebellum

Information Human

Age_Group	Sex	n	AOD	Braak	RIN	PMI
AD						
A	male	8	76.75 (± 2.25)	5.31 (± 0.46)	7.84 (± 1.15)	9 (± 8.72)
A	female	10	76 (± 3.13)	5.6 (± 0.52)	8.39 (± 0.86)	5.29 (± 4.82)
B	female	22	84.91 (± 2.76)	5.59 (± 0.53)	8.46 (± 0.72)	4.86 (± 3.03)
B	male	15	85.13 (± 2.03)	5.43 (± 0.62)	8.24 (± 0.9)	7.82 (± 5.62)
C	female	13	90+	5.42 (± 0.53)	8.41 (± 0.27)	15.71 (± 13.59)
C	male	7	90+	5.29 (± 0.49)	8.13 (± 0.59)	11.5 (± 7.68)
PSP						
A	female	21	75.48 (± 3.76)	2.1 (± 0.89)	8.68 (± 0.91)	7.78 (± 6.22)
A	male	29	75.28 (± 3.06)	2.12 (± 0.91)	8.22 (± 0.97)	8.75 (± 7.4)
B	female	3	82.33 (± 2.31)	1.17 (± 1.26)	8.07 (± 0.97)	11.33 (± 2.08)
B	male	9	84.11 (± 2.37)	2.39 (± 0.99)	8.3 (± 0.9)	3.5 (± 0.71)
Control						
A	female	3	76.67 (± 2.08)	-	7.5 (± 1.05)	2.67 (± 1.15)
A	male	13	76.15 (± 2.85)	-	7.57 (± 1.18)	3.75 (± 3.93)
B	female	21	85.86 (± 2.2)	-	7.54 (± 1.02)	4.24 (± 3.01)
B	male	16	85.12 (± 2.99)	-	7.64 (± 0.94)	5.71 (± 5.55)
C	male	7	90+	-	8.49 (± 0.64)	13.8 (± 11.32)
C	female	10	90+	-	7.1 (± 1.02)	13.89 (± 11.33)

AOD = Age of Death, **n** = number of samples, **RIN** = RNA integrity number, **PMI** = Postmortem interval (in hours).
ALZ = Alzheimer Disease.
PSP = Progressive Supranuclear Palsy.
Values are mean ± SD.

Table 3. Summary of technical variables of samples from 5XFAD and TauD35 data.

Information 5XFAD - Model			
Age_Group	Sex	n	RIN
HIP - Control			
4 M	female	10	9.58 (± 0.26)
4 M	male	10	9.09 (± 0.73)
12 M	male	12	-
12 M	female	8	9.89 (± 0.1)
18 M	male	8	-
18 M	female	32	-
HIP - Alzheimer			
4 M	female	10	9.73 (± 0.19)
4 M	male	10	9.62 (± 0.27)
12 M	male	8	9.89 (± 0.08)
12 M	female	10	9.73 (± 0.21)
18 M	male	20	-
18 M	female	12	-

M = Months, **n** = number of samples, **RIN** = RNA integrity number.
HIP = Hippocampus.
Values are mean ± SD.

Information TAUd35 - Model			
Age_Group	Sex	n	RIN
Alzheimer			
4 M	female	1	8.9
4 M	male	4	8.7 (± 0.29)
17 M	male	3	8.47 (± 0.23)
17 M	female	1	8.8
Control			
4 M	male	4	8.72 (± 0.15)
4 M	female	1	8.9
17 M	female	4	8.57 (± 0.3)
17 M	male	2	8.55 (± 0.49)

M = Months, **n** = number of samples, **RIN** = RNA integrity number.
Values are mean ± SD.

Table 4. Summary of clinical, demographich, and technical variables of samples of human MSBB data

BA10 - BA36

Information Human					
Sex	n	AOD	Braak	RIN	PMI
AD - BA10					
female	71	85.75 (± 6.07)	5.24 (± 1.16)	6.26 (± 1.48)	3.62 (± 2.27)
male	34	80.5 (± 7.95)	5.35 (± 1.1)	6.26 (± 1.43)	3.98 (± 2.58)
Control - BA10					
male	34	77.68 (± 8.56)	1.65 (± 0.95)	6.79 (± 1.09)	7.45 (± 4.47)
female	37	84.19 (± 6.66)	2 (± 1.05)	6.8 (± 1.04)	4.56 (± 3.03)
AD - BA36					
male	28	79.71 (± 8.69)	5.36 (± 1.1)	5.62 (± 1.68)	3.75 (± 2.52)
female	60	86.32 (± 5.67)	5.18 (± 1.24)	5.64 (± 1.7)	3.44 (± 2.42)
Control - BA36					
female	34	82.76 (± 8)	2.06 (± 1.2)	6.35 (± 1.31)	4.49 (± 3.25)
male	30	77.3 (± 8.78)	1.53 (± 0.86)	6.44 (± 1.16)	7.56 (± 4.67)

AOD = Age of Death, **n** = number of samples, **RIN** = RNA integrity number, **PMI** = Postmortem interval (in hours).
AD = Alzheimer's Disease.
BA = Broadmann Area.
Values are mean ± SD.